NJC

Accepted Manuscript

This is an *Accepted Manuscript*, which has been through the Royal Society of Chemistry peer review process and has been accepted for publication.

Accepted Manuscripts are published online shortly after acceptance, before technical editing, formatting and proof reading. Using this free service, authors can make their results available to the community, in citable form, before we publish the edited article. We will replace this *Accepted Manuscript* with the edited and formatted *Advance Article* as soon as it is available.

You can find more information about *Accepted Manuscripts* in the Information for Authors.

Please note that technical editing may introduce minor changes to the text and/or graphics, which may alter content. The journal's standard Terms & Conditions and the Ethical guidelines still apply. In no event shall the Royal Society of Chemistry be held responsible for any errors or omissions in this *Accepted Manuscript* or any consequences arising from the use of any information it contains.

ROYAL SOCIETY OF CHEMISTRY

www.rsc.org/njc

Multifunctional Composite of Antibacterial Higher-valent Silver Metallopharmaceutical and Potent Wound Healing Polypeptide: A Combined Killing and Healing Approach to Wound Care

Sukdeb Pal[1, 2, †], *Yu Kyung Tak*[1, †], *Eunyoung Han*[3], *Sabarinathan Rangasamy*[1], *Joon Myong Song*[1,*]

[1]*Research Institute of Pharmaceutical Sciences and College of Pharmacy, Seoul National University, Seoul 151-742, South Korea*

[2]*CSIR-National Environmental Engineering Research Institute, Nehru Marg, Nagpur 440-020, India*

[3]*College of Pharmacy, Duksung Women's University, 33, Samyangro 144-gil, Dobong Gu, Seoul, South Korea*

† These authors have contributed equally

* Corresponding author

Prof. Joon Myong Song

Tel.: 82-2-880-7841, Fax: 82-2-871-2238, E-mail address: jmsong@snu.ac.kr

Abstract:

The present study relates to a combined killing and healing approach for treatment of infected wound. Herein we report a multifunctional, including antimicrobial and wound healing, composite containing a conjugate of a bi-valent silver polydiguanide that demonstrated high antibacterial activity *in vitro* and a potent wound healing polypeptide, histatin-1, for treatment of infected wound. Synthesis of silver (II) chlorhexidine [Ag(II)CHX] was accomplished by oxidation of Ag(I), followed by complexation of the oxidized metal with chlorhexidine (CHX), whereas the metal complex conjugate of solid phase-synthesized Histatin polypeptide (Hst-1), Hst-1-[Ag(II)CHX], was realized by mixing the starting materials in aqueous solution. The change in Hst-1 structure upon binding with silver complex was examined by circular dichroism spectroscopy. Wound healing applicability of histatin polypeptide and its metal complex conjugate was tested using synthesized Hst-1 and Hst-1-[Ag(II)CHX] complex on 3T3-L1 preadipocytes in a cell-spreading assay. The antibacterial activity of the silver metal complex and its Hst-1conjugate was tested against several Gram positive and Gram negative bacteria, including Methicillin-resistant *Staphylococcus aureus* (MRSA) *and* Methicillin-resistant coagulase negative *staphylococcus* (MRCNS) by broth microdilution method. Results of these experiments revealed that polypeptide and silver(II) polydiguanide complex retained their individual wound healing and antimicrobial activity even in their conjugate. The conjugate of an antibacterial higher-valent silver polydiguanide complex with a potent wound healing polypeptide (Hst-1) showed promise as a new multifunctional therapeutic wherein the killing and healing functions of the constituent materials are preserved together, for development of new-generation wound-care agents.

Keywords: antibacterial agents, wound healing, polypeptides, higher-valent silver complex

Introduction:

The repair of wounds is one of the most complex biological processes that occur during human life. After an injury, multiple biological pathways immediately become activated and are synchronized to respond. Wound healing is a highly regulated, albeit poorly understood, process that probably involves: 1) inflammation, 2) cell proliferation and migration, angiogenesis, and 3) extracellular matrix (ECM) production.[1] In the first event neutrophils, monocytes, and lymphocytes accumulate in the wound area. During proliferation fibroblasts, endothelial cells, and other cell types migrate into the affected area and begin to proliferate, secrete matrix materials, and form functional capillaries, and layer of epithelial cells spreads over the open wound. Finally in the maturation phase skin collagen and other matrix materials are secreted and remodeled to restore tissue strength.[2-4]

To accelerate the healing processes in wound repair, attempts have been repeatedly made to use growth factors and their peptide fragments that can regulate most of these events, including the chemotaxis of inflammatory cells,[5] angiogenesis,[6] ECM deposition, and granulation tissue formation,[7] hereby promoting healing.

Apart from surgical procedures and irrigation, current therapeutic regimens often encompass local or systemic use of topical antimicrobials to help combat microorganism growth around the wound, and to provide suitable microenvironment for healing.[8] Previous literature, however, has pitted the potential significant benefits against the possible deleterious effects of many agents on the wound-healing process.[9-11]

Since pathogenesis of many diseases involve multiple factors and a selective compound against a single target often fails to achieve the desired effect, we speculated that developing multi-functional therapeutic combining an antimicrobial and a wound healing agent would further accelerate the healing processes in wound repair.

Salivary peptides represent a relatively new discovery in the immune system pathway. Recently Oudhoff et al.[12, 13] revealed a new and interesting activity of histatin, a salivary peptide family, which for decades had been primarily regarded as antimicrobial peptides implicated in the innate immunity of humans and higher primates.[14, 15] Histatin, isolated from human saliva, was identified as the component that was responsible for the *in vitro* epithelial-cell-migration-inducing properties of saliva.[13] These small peptides are inducible elements of the immune system that have been shown to enhance reepithelialization by stimulating cell-migration and cell-spreading. Reepithelialisation of full thickness wounds was enhanced by histatin-1 (Hst-1), Hst-2 [or (Hst-1(12–38)] and Hst-3, with rates comparable to those of the gold standard rhEGF. Histatin did not enhance proliferation but stimulated reepithelialization by stimulating cell migration and cell spreading, the two key initiating steps in reepithelialization. Hst-1 and Hst-2 (12-38 Hst-1) was identified as the most potent enhancers in *in vitro* wound closure assays, whereas Hst-5 the most potent antimicrobial of the histatin family did not show any wound healing property. Activation of cells by histatin requires a G-protein-coupled receptor that activates the ERK1/2 pathway.[12] These studies emphasize the role of histatin in tissue protection and recovery, and especially the importance of development of synthetic histatins as novel skin wound-healing agents. The other advantage of using histatins over the recombinant growth factors currently in clinical trials is that histatins are stable molecules and can be produced easily even on a large scale.[16] They therefore have a high potential for use as novel therapeutics suited for the treatment of wounds. The small size of Hst-1 or Hst-2 (12-38 Hst-1) makes this peptide a good candidate for transdermal delivery, and hence a potential therapeutic agent for wound healing.

Traditional topical agents, especially silver and silver-based compounds such as silver sulfadiazine have been well documented in the literature regarding their use and benefit in wound care.[17] However, these agents can present particular difficulties related to resistance or

inhibition of the wound-healing process. The use of silver sulfadiazine, for example, has been demonstrated to increase wound epithelialization but can impair wound contraction.[18] Other antibacterial agents such as Sulfamylon has been demonstrated to enhance angiogenesis, epithelialization, and dermal thickening in some studies, whereas in others it has been linked to decreases in keratinocyte growth rates and is a known source of acidosis through its inhibition of carbonic anhydrase.[9, 19] In addition, these agents have limited spectra of antibacterial activity.[20, 21] Other topical agents such as Dakin's solution, Betadine, acetic acid, and hydrogen peroxide used to decrease wound bacterial load either have deleterious effects on fibroblasts and endothelial cells at traditionally used concentration or impair neutrophil migration and wound neovascularization[22] or slow down the rate of reepithelialization and impair microcirculation at higher levels of concentration.[23] This has prompted an upsurge in research on the synthesis of silver complexes with improved antibacterial activity especially against multidrug resistant bacteria.[24-26] In an interesting development, Melaiye et al.[27] showed that bactericidal activity of ionic silver is correlated to its valence form and it has been found that higher valence silver demonstrates stronger and effective antibacterial activity than lower valence ion.[28-30] Recently, we reported a nanocrystalline tri-valent silver polydiguanide metallopharmaceutical that showed much higher antibacterial activity than the gold standard, silver sulfadiazine, against a wide variety of bacteria methicillin-resistant *Stahylococcus aureus* (MRSA) strains in *in vitro* studies.[31] However, they are difficult and expensive to produce in large quantities. Large scale synthesis of stable higher-valent silver metallopharmaceuticals in terms good hydration, sustained release of silver ions with increased concentration at the wound surfaces and most importantly low toxicity will be pivotal in infected wound care.

The newly discovered wound healing function of Hst and highly antibacterial character of higher-valent silver complexes prompted us to combine these two agents in to a

multifunctional therapeutic, and verify the possibility of using our killing and healing approach in wound care. To achieve this objective we first developed one-pot method for large scale synthesis of a di-valent silver polydiguanide complex that showed strong antibacterial activity against the tested Gram (+)/(-) strains. Finally, we investigated the possibility of combining the synthesized complex and synthesized Hst in one form as a better multifunctional therapeutic for infected wound care. The individual activity of the metal complex and the peptide was assayed after combination and this revealed that the combination has no effect on their individual biological activities. This work identifies the combination of higher-valent silver complex and synthetic histatin as a potent multifunctional wound-healing agent, which may form the basis of a novel wound-healing medication.

Materials and Methods:

Peptide synthesis

Linear peptide (Hst-1, amino acid sequence DSHEKRHHGYRRKFHEKHHSHREFPFYGDYGSNYLYDN) was synthesized by solid-phase peptide synthesis using Fmoc chemistry with an automatic peptide synthesizer (AnyGen, Jeollanam-do,Korea). The product was purified using RP-HPLC, and the authenticity was confirmed by mass spectrometry (4848 Da).

Synthesis of silver (II) chlorhexidine complex [Ag(II)CHX]

A 0.49 mmol portion of chlorhexidine (1,1'-hexamethylenebis [5-p-chlorphenyl] biguanide) (0.25 g) was dissolved in 20 mL dimethyl sulfoxide (DMSO). To this solution an aqueous solution (1.25 mL) containing 0.5 mmol of silver nitrate (0.085 g) was added drop wise while stirring the reaction mixture continuously. This was followed by addition of 1.25 mL aqueous solution containing 0.99 mmol portion of sodium persulphate (0.235 g). The reaction mixture

was allowed to remain under stirring condition for at least 10 minutes. Subsequently, 20 mL water was added to the reaction mixture. The reaction mixture was again stirred for at least 1 minute and was allowed to stand for at least 4 hours at room temperature to yield a brown precipitate which was filtered under vacuum, washed with water, and dried at ambient temperature to obtain microcrystalline silver (II) chlorhexidine complex [Ag(II)CHX]. The reaction is schematically shown in Figure 1a.

Synthesis of Hst-1-[Ag(II)CHX] complex conjugate

Lyophilized histatin-1 (Hst-1) was reconstituted by dissolving it in 20 mM phosphate buffer at pH 7. Working solutions were obtained by diluting this stock with phosphate buffer medium. The Hst-1-[Ag(II)CHX] complex conjugates with different peptide and metal complex molar ratios were realized by adding the DMSO solution of [Ag(II)CHX] to the aqueous solution of Hst-1 followed by incubation of the reaction mixture at least for 1h at 2-8^{0}C. The Hst-1-[Ag(II)CHX] complex conjugate solution with desired peptide-metal complex molar ratio was stored at 2-8^{0}C at least for 1 month for further use *in vitro* antibacterial susceptibility tests and cell-spreading assays.

^{1}H-NMR spectroscopy of CHX and [Ag(II)CHX]

Proton NMR spectra were recorded at 500 MHz using a Bruker AMX 500 FT-NMR spectrometer. All spectra were obtained in DMSO-d_6. Chemical shifts are reported in δ (ppm) units relative to tetramethylsilane. The details and results of the ^{1}H-NMR analyses of CHX and [Ag(II)CHX] are presented below.

^{1}H-NMR (DMSO-d_6) δ for CHX (500 MHz): 7.19 (d, 4H, Ar H), 6.79 (d, 4H, 2H; Ar H), 4.84 (s, 2H; Ar C-NH), 3.99 (s, 4H, C=NH), 3.10 (s, 4H, NH), 1.44 (4H, CH_2), 1.31 (4H, CH_2), 1.23 (4H, CH_2).

^{1}H-NMR (DMSO-d_6) δ for [Ag(II)CHX] (500 MHz): 7.35 (8H, Ar H), 3.99 (s, NH_2), 1.44 (4H, CH_2), 1.25 (4H, CH_2), 1.14(4H, CH_2); Anal. calcd for $[Ag(C_{22}H_{30}AgCl_2N_{10})](OH)_2.2H_2O$: C, 38.67; H, 5.31; Ag, 15.78; N, 20.50; found: C, 38.81; Ag, 15.64; H, 4.95; N, 20.59.

X-ray photoelectron spectroscopy of [Ag(II)CHX]

Surface chemistry was analyzed by XPS (Sigma Probe, Thermo-VG, UK) with monochromatic Al Kα (1486.7 eV) X-ray source. Survey XPS data were acquired over 1200 eV in Constant Analyzer Energy mode with pass energy of 30 eV and a resolution of 0.1 eV.

Circular dichroism spectroscopy of Hst-1 and Hst-1-[Ag(II)CHX] conjugate system

Circular dichroism (CD) spectra were measured with a Jasco J 600 CD spectropolarimeter (Jasco, Tokyo, Japan) calibrated with camphorsulfonic acid. Spectra were recorded between 200 and 250 nm using a path length of 0.1 cm, a time constant of 1.0 s, a 2 nm bandwidth and a scan rate of 2 nm per min, and at 20 or 50 mdeg. The average was corrected by 4 scans of the solvent. Quartz cell (0.1cm path length) sealed and controlled thermostatically were used for the far-UV CD measurements. The spectra in the presence of varying amount of 2, 2, 2-trifluoroethanol (TFE) (0, 10, 20, 30, 50 and 70%) and varying concentrations of [Ag(II)CHX] (0, 2, 5, 10, 20, 30, 40 µM dissolved in TFE) were collected at a concentration of 20 and 40 µM Histatin-1 (dissolved in 20 mM phosphate buffer at pH 7), respectively. To investigate the effect of varying amount of TFE (5, 10, 20, 30, 40, 50, 60, 70%) on the Hst-1-[Ag(II)CHX] conjugate system the spectra were collected using a equimolar (20 µM) mixture of Histatin-1(dissolved in 20 mM phosphate buffer, pH 7) and [Ag(II)CHX] (dissolved in TFE).

Cell-line culture

3T3-L1 preadipocytes were obtained from the Korean Cell Line Bank (KCLB, Seoul, Korea) and cultured in Dulbecco's modified Eagle's medium (DMEM) containing 10% (v/v) heat-inactivated fetal calf serum in an incubator of 5% $C0_2$, 37°C. The cell medium was exchanged at every 3 days. At this time, if more than 90% of cells were grown in the dish, the cells are serum-depleted by DMEM, not including 10% FBS, for 24 hours. After that the medium in the tissue culture flask were taken out with a pipette, and then the cells were washed by PBS and treated by 0.5% trypsin to take off the cells. The cells, collected by centrifugation in 1,000 × g for 3 minutes, were diluted again in culture medium to have 5×10^5 cells per 1 mL. At this time, cell number was measured using a hemocytometer.

In vitro cell-spreading assay

Cell-spreading assay was performed using 35mm μ-dish with two well culture–insert (ibidi GmbH, Munich, Germany). 70 μL of the cell suspension (5×10^5 cells per 1 mL) was seeded into each well. The outer area was filled with 150 μL cell free medium. After 36 h of cell adherence the culture-insert was gently removed by using sterile tweezers to create a cell-free gap of 500 μm, and the medium was changed with fresh cell medium supplemented with different compositions of Hst-1, [Ag(II)CHX] and Hst-1-[Ag (II) CHX] and without anything in case of control. Cell-spreading into the gap region was observed, and the images of each μ–Dish was taken at a time interval of 0h, 12h, and 24h using an optical microscope equipped with a charged coupled device (CCD) camera. The cell-free gap was calculated using commercially available image processing software (MetaMorph, Version 7.1.3.0, Molecular Devices). The relative cell-free area at a given time "*t*" (RG_t) was calculated as:

$$RG_t = \frac{G_t}{G_0} \times 100$$

where G_t is the cell-free gap area at time *t* and G_0 is the cell-free gap area at time 0.

Relative spreading (RS_t) was calculated as:

$$RS_t = \frac{G_0 - G_t}{G_0} \times 100$$

Evaluation of antibacterial performances of [Ag(II)CHX] and Hst-1-[Ag (II) CHX]

The test organisms include 4 strains of Gram-negative bacteria: *Acinetobacter calcoaceticus* (ATCC 23055), *Citrobacter freundii* (ATCC 6750), *Klebsiella pneumonia* (ATCC 10031) and *Pseudomonas aeruginosa* (ATCC 27853); 4 strains of Gram-positive bacteria: *Enterococcus faecalis* (ATCC 29212), *Staphylococcus aureus* (ATCC 25923), *Staphylococcus epidermidis* (ATCC 12228), and *Propionibacterium acnes* (ATCC 6919). All challenge bacterial strains were obtained from American Type Culture Collection (ATCC, Rockville, MD, USA) except for *P. acnes* ATCC 6919 which was provided by Korean Collection for Type Cultures (Daejon, Korea). All tests were performed in line with Clinical and Laboratory Standards Institute (formerly National Committee for Clinical Laboratory Standard, NCCLS) guidelines. The overnight cultures served as the inocula for experiments. Unless otherwise stated, the strains were grown overnight in Tryptic Soy broth or agar (TSB or TSA, Difco Laboratories, Detroit, MI, USA) at 37℃ under aerobic conditions. *P. acnes* (ATCC 6919) inocula were cultured in Brain Heart Infusion broth or agar (BHI, Difco Laboratories, Detroit, MI, USA) supplemented with 1% glucose (BHIG). They were grown for 48 h at 37℃ under anaerobic conditions created by the GasPak jar system (BBL Microbiology Systems, Cockeysville, MD).

Minimal inhibitory concentrations (MICs) of [Ag(II)CHX] and Hst-1-[Ag (II) CHX] composite were determined by the agar dilution method in BHI agar for *P. acnes* or in Mueller Hinton agar (MH, Difco Laboratories, Detroit, MI, USA) for all the other species,

using a multi-point inoculator. Plates were read after incubation at 37 ^{o}C for 48 hours under anaerobic conditions (GasPak) for *P. acnes*, or for 24 hours in air for all the other species. To determine the MICs by the broth microdilution method, Mueller Hinton broth (MH, Difco Laboratories, Detroit, MI, USA) was used for all bacterial strains except for *P. acnes* ATCC 6919, which was grown in BHI broth supplemented with 1% glucose. Strains were cultured in 96 well microplates. To evaluate the inhibitory effects of [Ag(II)CHX] and Hst-1-[Ag (II) CHX] composite on bacterial growth, each well was supplemented with a range of concentrations of the active agents. Following 24 hours incubation in air or 48 hours incubation in GasPak jar system at 37 ^{o}C, the wells were inspected for microbial growth and the MIC was determined as the lowest concentration that did not produce visual growth.

Results:

Characterization of [Ag(II)CHX]

The wet chemical preparation of [Ag(II)CHX] was realized by oxidizing the silver (I) (dissolved in aqueous medium) in presence of CHX (dissolved in DMSO) using an aqueous solution of sodium persulphate. Finally the complex [Ag(II)CHX] was precipitated from the feebly acidic or neutral medium (Fig. 1a).

FTIR and ^{1}H NMR spectra of CHX and [Ag(II)CHX] are depicted in Fig. 1b and c. The characteristic stretching bands at 3474 and 3408 cm^{-1} for –N(H)– as seen in CHX appeared as a single band in the complex. The signal at 4.84 ppm seen in the NMR spectrum of the ligand (CHX) is absent in NMR spectrum of the complex. These results indicate that the binding is due to the interaction between the nitrogen of the –N(H)– bond of CHX and silver.

The oxidation state of the metal in [Ag(II)CHX] was confirmed using X-ray photoelectron spectroscopy (XPS). The XPS spectrum of [Ag(II)CHX] is shown as Figure 1d. The spectrum clearly indicates the presence of Ag^{2+} in the complex. The characteristic Ag3d XPS

spectrum of [Ag(II)CHX] displays the presence of the Ag $3d_{3/2}$ and Ag $3d_{5/2}$ XPS peaks at 374.3 eV and 368.4 eV, respectively. These values fall in the range of literature values for Ag^{2+}.[32, 33]

Characterization of Hst-1 and Hst-1-[Ag(II)CHX] conjugate system

The circular dichroism (CD) spectra of Histatin-1 (dissolved in 20 mM phosphate buffer at pH 7) were recorded in the presence of varying amount of 2, 2, 2-trifluoroethanol (TFE) and varying concentrations of [Ag(II)CHX] (dissolved in TFE). The CD spectra of histatin-1 in aqueous medium (20 mM phosphate buffer, pH 7) or in aqueous solution/2, 2, 2-trifluoroethanol (TFE) mixtures are reported in Figure 2a. The dichroic profile indicates that the peptide assumes a random coil conformation in aqueous medium. Increasing the concentration of TFE caused a substantial increase in negative ellipticity at 208 nm ($\pi \rightarrow \pi^*$ transition) and at 222 nm ($n \rightarrow \pi^*$ transition), indicating the formation of a α-helix. The alpha sheet formation and stabilization appears at 50% TFE (v/v). A gradual increase of the helix content was observed with increasing TFE concentration. The effects of the presence of [Ag(II)CHX] on CD spectra of Histatin-1 were investigated in order to reveal the ability of the metal complex to induce conformational changes on histatin-1 (Fig. 2b). The minima of molar ellipticity of Histatin-1 appear at 200 nm which is a typical behavior of random coil peptide (Fig. 2b). Upon titration with [Ag(II)CHX], this pattern does not change. However, at an equimolar concentration of Histatin-1 and [Ag(II)CHX] maximum molar ellipticity was obtained. Consequently, the equimolar concentration of Histatin-1 and [Ag(II)CHX] was used in further experiments.

In the presence of 50% TFE, a tendency to produce a CD profile which is characteristic of helical conformation is seen (Fig. 2c). Addition of [Ag(II)CHX] was also investigated in order to reveal the effects of the metal complex on the conformation of this peptide. At an

equimolar concentration of the peptide and metal complex stabilization took place, and not much change was observed even after addition of excess of [Ag(II)CHX] (Fig. 2c). The effect of varying amount of TFE on the Hst-1-[Ag(II)CHX] conjugate system were investigated by collecting the CD spectra of a equimolar (20 µM) mixture of Histatin-1(dissolved in 20 mM phosphate buffer, pH 7) and [Ag(II)CHX] (dissolved in TFE). As shown in Figure 2d the addition of TFE to the complex of histatin-1 and [Ag(II)CHX] induced changes in the CD profile that is typical of a helical conformational change, characterized by the appearance of two minima at 208 and 222 nm. Moreover, in the presence of TFE the CD profile of Hst-1-[Ag (II) CHX] complex (Fig. 2d) does not change with respect to that of only Histatin-1(Fig. 2a).

Antibacterial susceptibility tests

The antibacterial properties of [Ag(II)CHX] and Hst-1-[Ag (II) CHX] conjugate were tested against Gram-positive and Gram-negative prokaryotes of clinical interest. The MIC values presented in Table 1 were determined using a broth microdilution method. The compounds of interest [Ag(II)CHX] showed better antibacterial activity than the free ligand (CHX), $AgNO_3$ and silver sulfadiazine (AgSD) even at much lower concentration (Table 1). MIC of the Ag(II)CHX for different bacteria strains tested ranged from 0.12-2 mg/L, which corresponds to 0.18-3µM. [Ag(II)CHX] almost quantitatively retained its antibacterial activity in presence of Hst-1. The MIC values of [Ag(II)CHX] alone and in presence of Hst-1 were much lower than those of CHX, $AgNO_3$, and AgSD, once again indicating the superior efficacy of [Ag(II)CHX] and Hst-1-[Ag(II)CHX] conjugate over the other tested compounds as an antibacterial agent. The minimum bactericidal concentrations (MBC) were determined to evaluate the bactericidal properties of [Ag(II)CHX] and in presence of Hst-1 (Table 1). In all antimicrobial tests, the free ligand CHX, and silver nitrate were used as the reference

317 standards. All test compounds, CHX, [Ag(II)CHX] (alone and in presence of Hst-1) and
318 $AgNO_3$ appeared to be bactericidal with MBC/MIC ratios of 1-2.
319
320 ***Wound healing activity test through in vitro cell-spreading assay***
321 Previous studies show that histatin promotes cell spreading and cell migration but does not
322 enhance cell proliferation.[7, 8] Cell spreading, which precedes migration, is very important for
323 reepithelialization. Our next aim was to investigate whether [Ag(II)CHX] affects the cell-
324 spread promoting property of the peptide. Therefore, we tested the effect of [Ag(II)CHX] on
325 the on cell-spreading activity of Hst-1 in presence or absence of equimolar (0.2-5μM) amount
326 of [Ag(II)CHX]. The concentrations of Ag(II)CHX were selected to cover the entire range of
327 MIC values of the complex (0.12-3 μM) as found in the *in vitro* antibacterial studies (Table
328 1). Representative microscopic images from the cell-spreading assays are shown in Figure 3.
329 The dose-response effect of [Ag(II)CHX], Hst1, and Hst-1[Ag(II)CHX] on cell-spreading
330 was examined by quantifying the cell free gap from microscopic images taken at different
331 time intervals using MetaMorph (Version 7.1.3.0, Molecular Devices). The results clearly
332 show that [Ag(II)CHX] did not enhance cell-spreading (Fig. 3a), neither had it impaired the
333 cell-spread promoting activity of the Hst-1 (Fig. 3b). As evident from the calculated relative
334 cell-free gap (RG_t) at different time interval, Hst-1-[Ag (II) CHX] conjugate promoted cell-
335 spreading with comparable values to those of equimolar concentration of Hst-1 (Fig. 3c).
336 Synthesized Hst-1 in absence or in presence of equimolar amount of AgHCX enhanced cell-
337 spreading in a dose dependent manner. While relative cell-spreading (*RGs*) in presence of 0.2
338 μM Hst-1 was comparable to the control, at higher concentration the relative cell-spreading
339 increased sharply with in first 12 h and complete cell coverage was achieved much faster than
340 the control (Fig. 3d).
341

Discussions:

Infected and colonized wounds impose a serious burden to entire health care system. While chronic wounds invariably involve a multitude of bacterial species, acutely infected wounds are more frequently resulted from the isolated or few species. Topical antimicrobials are often used to decrease the bacterial burden on infected tissue. Ideally topical agent should be extremely active against pathogens and have a neutral or even beneficial effect on the wound-healing process. Effective antimicrobial choices are therefore needed as drug resistance continues to emerge.

Among the inorganic antibacterial agents metallic silver, silver salts (e.g., $AgNO_3$), and silver complexes have been employed most extensively to fight infections and control spoilage in a variety of pharmaceutical and health care applications including post-operative wound management and burn wound treatment. Our group has longstanding interest in synthesis, biochemical properties of nanosilver and silver compounds with projected antibacterial applications. [31, 34, 35]

Although silver itself has low toxicity and medically has only one rare cosmetic side effect [36, 37] toxicity of silver compound has often been associated with the carrier molecules. Therefore, coordination of silver to other nontoxic molecules could offer a solution for safe use of silver compounds as antimicrobials. Biologically compatible molecules known to have minimal or no established in vivo toxicity, such as polydiguanides that have attracted considerable attention as highly efficient biocidal and nontoxic agents,[38] may be excellent candidates for this purpose. Interestingly, biguanide or substituted biguanide, such as ethylenebiguanide, forms quadricovalent cationic complexes with Ag(III) that are stable (including photostable) in ambient conditions. In the present study, we chose a commonly used symmetric polydiguanide molecule, chlorhexidine, 1,1′-hexamethylene-bis-5-(4-chlorophenyl)biguanide, with two ionizable guanide moieties as the ligand to synthesize stable silver complex.

Biguanides are well known ligands capable of forming strong complexes with both metals and nonmetals. LCAO-MO calculations show that they possess delocalized π-electron system in neutral or basic medium in the free state as well as in complexes. Further delocalization of this π-electron system through the vacant metal *d*-orbitats in metal chelates gives rise to strong metal-ligand bonding. In the complexes of these ligands with metal ions in normal oxidation state, some of metal *d*-electrons may be raised to high energy antibonding orbitals due to overlapping of filled ligand orbitals with the metal *d*-orbitals. This facilitates the removal of metal *d*-electrons favoring higher oxidation states of metals. The resulting metal complexes in high oxidation state may further be stabilized by the flow of π-electron density from the filled ligand orbitals to vacant metal *d*-orbitals and thus reducing the electronegativity of the metal to a great extent.

Chlorhexidine (CHX) is also an important antiseptic, disinfectant, pharmaceutical and cosmetic preservative and antiplaque agent. The free base is essentially water insoluble and only exists at very low hydrogen ion concentrations (pH > 12). It is used in salt form and commercially available as diacetate, dihydrochloride, or digluconate. However, considering the undesirable interaction of metal ion with other organic species and precipitation of AgCl, these salts of CHX are not the best choices as ligand source. In our earlier studies,[31,35] taking advantage of the pK_a values of CHX (2.2 and 10.3), which make it dicationic over the entire range of physiological pH,[39] the ligand (CHX) was solublized in water by forming a dihydrogensulfate salt of it in acidic medium. The higher-valent silver complex was produced by the removal of some of the metal *d* electrons by the peroxydisulfate oxidation from the higher-energy antibonding orbitals of the Ag(I) complex. The feebly acidic or neutral medium most appropriate for complexation was provided by addition of bicarbonate. Unlike the previous method developed by us, [31, 35] in this study CHX were solublized in DMSO. This has two fold advantages. First, low pH is avoided, and the reaction can actually proceed in

feebly acidic medium, and secondly it eliminates the need of addition of base (bicarbonate) for final pH adjustment. Once the bi-valent silver complex is produced by peroxydisulfate oxidation, precipitation of the complex can be easily achieved by simple addition of water to the reaction mixture.

FTIR and ^{1}H NMR spectra of CHX and [Ag(II)CHX] are depicted in Figure 1b and c. FTIR and ^{1}H NMR studies show that binding is due to the interaction between the nitrogen of the –N(H)– bond of CHX and silver. Both FTIR and NMR spectra of [Ag(II)CHX] are very similar to that of a tri-valent silver complex we reported earlier.[31] Few attempts have been made for probable assignments of bands for biguanide and its metal complexes.[40, 41] The band positions for ν(-NH-) in (C=NH) and in (C-NH_2) for the ligands are very difficult to identify due to the presence of electron delocalization in the ligand. This will be more complicated due to the presence of water molecules. Peaks appearing in the region 3500-3000 cm^{-1} in the ligand as well as in the complexes may be due to ν(-NH-) in (C=NH) and (C-NH_2) or ν(-OH) (from H_2O) groups. The characteristic stretching bands at 3474 and 3408 cm^{-1} for –N(H)– appeared as a single band in the complex. The absence of signal at 4.84 ppm in the complex provides further support in favor of this bonding mode.

Similarly bands in the region 1680-1430cm^{-1} may be due to ν (N-C-N) and δ (NH_2). In this region (1600-1430 cm^{-1}) 4 bands are observed at around 1660 cm^{-1}, 1600 cm^{-1}, (1530-1540) cm^{-1} and 1480cm^{-1}. The middle one appears at 1605 cm^{-1} in the free ligand and at 1580 cm^{-1} in complexes may be most likely due to δ (NH_2). This band position is not sensitive to the oxidation state of the metal atom. The band at 1666 cm^{-1} assigned to ν (N-C-N) shows a considerable red shift (1637cm^{-1}) in complex. This red shift may be due to drift of π-electron density from ligand towards the positive metal ion. In case of highly oxidized metal ion, the electron density drift will cause a further red shift.

The oxidation state of the central metal ion was confirmed by XPS. The binding energy data fall in the range of values reported for a number of Ag (I) and Ag (II) complexes. [32, 33]

The mobility in the peptide structure in TFE can be explained considering the aqueous and lipophilic nature of the system. In fact, an increase of helix content was observed in CD spectra with increase in TFE concentration (Fig. 2). As shown in Figure 2c the addition of [Ag(II)CHX] to histatin-1 in presence of TEF induces changes in the CD profile characteristic of a helical conformational change, characterized by the appearance of two minima at 208 and 222 nm. In their study of interactions of the Aβ1-40 amyloid peptide with zinc ions Huang et al.[42] found that solvents are able to promote α-helical conformations favoring peptide-metal interactions. It is noteworthy that in the 3_{10}-helix the (n→π*) transition exhibits a drastically reduced intensity with respect to that of the (π→π*) transition and tends to undergo a modest blue shift.[43] Values for the $[\theta]_{222}/[\theta]_{208}$ ratio close to unity are seen as typical of the α-helix; a value of 0.15-0.40 is considered diagnostic for the 3_{10}-helical conformation. In our case, the $[\theta]_{222}/[\theta]_{208}$ ratio is 0.07 in 20 mM phosphate buffer (pH 7), 0.81 in 50% TFE and 0.83 in the presence of 20 μM [Ag(II)CHX], indicating a better stabilization of the right-handed α-helix in TFE medium and in presence of [Ag(II)CHX].

Determination of minimal inhibitory concentration (MIC) is a standard microbiological technique used to evaluate the bacteriostatic activity of antimicrobial agents. It is important to state that the theoretical amount of silver ions that could be released from 1 g of [Ag(II)CHX] is about 2 times lower than that from 1 g of silver nitrate and AgSD. Theoretically the antimicrobial activity of silver ion can be considered to be a combination of active silver species, which may include anionic silver halide ions, clusters of Ag^+ ions, and AgCl (formed at the initial stage). While anionic silver dichloride is known to be soluble in aqueous media and thus is bio-available,[44] and anionic silver halides are toxic to both sensitive and resistance strain bacteria,[45] precipitation of AgCl out of the media decreases the bioavailability of silver.

Broth solution contains ~ 86 mM NaCl. As observed in the present study, the lower activity of $AgNO_3$ and AgSD compared to [Ag(II)CHX] in liquid broth can be attributed to the precipitation of AgCl, i.e., lower availability of silver in the supernatant solutions. Therefore, we may speculate that [Ag(II)CHX] reacts more slowly with the chloride ions than silver nitrate or AgSD in the growth medium. The contribution of the polydiguanide ligand, therefore, appears to be significant toward reducing the formation of silver chloride in the broth solution compared to silver nitrate. Silver polydiguanide complexe [Ag(II)CHX] seems to be more stable than silver nitrate in chloride-containing medium. This is an excellent property considering the potential *in vivo* application of silver polydiguanide complexes.

Histatins are a family of at least 12 histidine-rich cationic peptides encoded by the *Htn1*and *Htn2* genes that are specifically expressed in human salivary glands.[46] Hst-1 is the primary gene product of *Htn1*, and Hst-2 is a shorter variant, which probably originated from Hst-1 by intracellular processing before secretion. The other histatins are products of *Htn2* of which Hst-3 and Hst-5 are most abundant in saliva. Together, Hst-1, Hst-3, and Hst-5 comprise ~ 85% of the total of histatin proteins. It has become clear that besides their antimicrobial functions, a number of these peptides also have effects on the tissue of the host. Like other antimicrobial peptides present in human saliva (such as defensins and LL-37) histatins also have growth stimulating properties.[47, 48] However, unlike LL-37 and defensins which act via direct or indirect activation of EGFR,[49, 50] histatins activate the cells independently from the EGFR. The interaction of histatin with its target cells displays characteristics that resemble those of regular growth factors, such as EGF, which on binding are taken up by endocytosis. The active uptake of Hst-1 likely occurs via a stereospecific receptor. Moreover, while LL-37 and defensins are cytotoxic at somewhat higher concentrations, [50] and activate cells in a narrow concentration range, histatins were reported to induce wound closure within a range from 5 to 100 µg/ml without showing any cytotoxicity. Our finding that Hst-1 promoted cell-spreading

in the tested concentration range (0.2 – 5 µM) is also in line with the previous findings. The mechanism of action of histatin is essentially different from that of LL-37.

Previous studies also revealed that stimulating activity of Histatin on host cells involves a stereospecific interaction with a putative membrane receptor.[7, 8] The fact that the D-enantiomer of Hst-2 (12-38 Hst-1) did not induce wound closure indicates stereospecific activation. Since the ligand used for synthesis of [Ag(II)CHX] has a high protein binding value we thought that it might impair the activity of the Hst-1 in presence of [Ag(II)CHX] , or in other words, the antibacterial activity of [Ag(II)CHX] might get reduced upon conjugation with Hst-1. However as shown in the Fig. 3 and Table 1, the individual biological activity of both Hst-1 and [Ag(II)CHX], remained almost unchanged in presence of each other. This interesting result provided a valuable inspiration to further work on development of multifunctional medication for infected wound care based on our combined killing-and healing approach.

Conclusion:

The possibility of combining an antimicrobial agent and a wound healing promoter into a multifunctional therapeutic for treatment of infected wound was explored in the present study. This was achieved by first developing an one-pot method for large scale synthesis of an antibacterial di-valent silver polydiguanide complex [Ag(II)CHX], and then combining this metal complex with a potent wound healing polypeptide, Hst-1. Both the synthesized di-valent silver complex [Ag(II)CHX] and its conjugate with Hst-1 demonstrated much better *in vitro* antibacterial activity against several Gram positive and Gram negative bacteria, including Methicillin-resistant *Staphylococcus aureus* (MRSA) and Methicillin-resistant coagulase negative *staphylococcus* (MRCNS) than the mono-valent silver compounds like gold standard silver sulfadiazine or silver nitrate, and only polydiguanide (chlorhexidine)

ligand. As revealed by the *in vitro* cell-spreading assay the histatin polypeptide-silver polydiguanide complex conjugate also appeared to be beneficial as a wound healing promoting agent. We believe that this combined killing and healing approach using a higher vlent silver based antimicrobial agent and a wound healing polypeptide showed significant promise as a new therapeutic for treatment of infected wound. However, it is imperative that the effects of the developed multifunction therapeutic on vascularization, contraction, epithelialization, and so forth, as has been accomplished with other antimicrobials in clinical trials over the years, be explored for future use in infected wounds.

Funding:

This work was supported by the National Research Foundation of Korea (NRF) grant funded by the Ministry of Education, Science and Technology (MEST) (2012-0005653 and 2008-0061858). We are grateful to the Research Institute of Pharmaceutical Sciences at Seoul National University for providing some experimental equipment.

Transparency declarations:

None to declare.

References:

1 Clark RAF: Overview and general consideration of wound repair. The Molecular and Cellular Biology of Wound Repair. New York: Plenum Press,1996; 3–50

2 G. C. Gurtner, S. Werner, Y. Barrandon and M. T. Longaker, *Nature*, 2008, **453**, 314-32.

3 A. S. Colwell, M. T. Longaker and H. P. Lorenz, *Front. Biosci.*, 2003, **8**, s1240–1248

4 Regan MC, Barbul A. The cellular biology of wound healing. In: Schlag G. Redl H, eds. Wound Healing. Heidelberg: Springer-Verlag, 1994:3

5 S. M. Wahl, D. A. Hunt, N. M. Wakefield, N. McCartney-Francis, L. M. Wahl, A. B. Roberts and M. B. Sporn, *Proc. Natl. Acad. Sci. U. S. A.*, 1987, **84**, 5788–5792

6 A. B. Roberts, M. B. Sporn, R. K. Assoian, J. M. Smith, N. S. Roche, L. M. Wakefield, U. I. Heine, L. A. Liotta, V. Falanga, J. H. Kehrl and A. S. Fauci, *Proc. Natl. Acad. Sci. U. S. A.*, 1986, **83**, 4167–4171

7 R. A. Clark, G. A. McCoy, J. M. Folkvord, J. M. McPherson, *J. Cell. Physiol.*, 1997, **170**, 69–80

8 A. B. G. Lansdow, A. Williams, S. Chandler and S. Benfield, *J Wound Care*, 2005, **14**, 155-160.

9 Y. Q. Tang, J. Yuan, G. Osapay, K. Osapay, D. Tran, C. J. Miller and A. J. Quellette, *Science*, 1999, **286,** 498–502.

10 F. Niyonsaba, H. Ushio, N. Nakano N and W. Ng, *J. Invest. Dermatol.*, 2007, **127,** 594–604.

11 K. P. Xu, J. Yin and F. S. Yu, *Invest. Ophthalmol. Visual Sci.*, 2007, **48,** 636–643.

12 M. J. Oudhoff, K. L. Kroeze, K. Nazmi, P. A. van den Keijbus, W. van 't Hof, M Fernandez-Borja, P. L. Hordijk, S. Gibbs, J. G. Bolscher and E. C. Veerman, *FASEB J.*, 2009, **23**, 3928-35

13 M. J. Oudhoff, J. G. Bolscher, K. Nazmi, H. Kalay, W. van 't Hof, A. V. Amerongen and E. C. Veerman, *FASEB J.*, 2008, **22**, 3805-12

14 B. J. Baum, J. L. Bird, D. B. Millar and R. W. Longton, *Arch. Biochem. Biophys.*, 1976**,** **177,** 427–436.

15 F. G. Oppenheim, T. Xu, F. M. McMillian, S. M. Levitz, R. D. Diamond, G. D. Offner and R. F. Troxler, *J. Biol. Chem.*, 1988, **263,** 7472–7477

16 S. Barrientos, O. Stojadinovic, M. S. Golinko, H. Brem and M. Tomic-Canic, *Wound Repair Regen*, 2008, **16,** 585–601.

17 B. S. Atiyeh, M. Costagliola, S. N. Hayek and S. A. Dibo, *Burns*, 2007, **33**, 139-148.

18 S. Tokumaru, K. Sayama, Y. Shirakata, H. Komatsuzawa, K. Ouhara, Y. Hanakawa, Y. Yahata, X. Dai, M. Tohyama, H. Nagai, L. Yang, S. Higashiyama, A. Yoshimura, M. Sugai and K. Hashimoto, *J. Immunol.*, 2005, **175,** 4662–4668.

19 N. Zhou, Z. Luo, J. Luo, X. Fan, M. Cayabyab, M. Hiraoka, D. Liu, X. Han, J. Pesavento, C. Z. Dong, Y. Wang, J. An, H. Kaji, J. G. Sodroski and Z. Huang Z, *J. Biol. Chem.*, 2002, **277,** 17476–17485

20 W. E. Gayle, C. G. Mayhall, V. A. Lamb, E. Apollo and B. W. Jr. Haynes, *J. Trauma.*, 1978, **18**, 317–323.

21 E. C. III. Smoot, J. O. Kucan, D. R. Graham and J. E. Barenfanger, *J Burn Care Rehabil.*, 1992, **13**(2 pt 1), 198–202

22 L. L. Bennett, R. S. Rosenblum, C. Perlov, J. M. Davidson, R. M. Barton and L. B. Nanney, *Plast Reconstr Surg.*, 2001, **108**, 675–687

23 S. S. Brennan and D. J. Leaper, *Br J Surg.*, 1985, **72**, 780–782.

24 A. Melaiye, R. S. Simons, A. Milsted, F. Pingitore, C. Wesdemiotis, C. A. Tessier and W. J. Youngs, *J. Med. Chem.*, 2004**, 47**, 973-977.

25 S. Ray, R. Mohan, J. K. Singh, M. K. Samantaray, M. M Shaikh, D. Panda, P. Ghosh, *J. Am. Chem. Soc.*, 2007, **129**, 15042-15053

26 K. M. Hindi, T. J. Siciliano, S. Durmus, M. J. Panzner, D. A. Medvetz, D. V. Reddy, L.A. Hogue, C. E. Hovis, J. K. Hilliard, R. J. Mallet, C. A. Tessier, C. L. Cannon and W. J. Youngs, *J. Med. Chem.*, 2008, **51**, 1577-83

27 A. Melaiye, Z. Sun, Z. Hindi, A. Milsted, D. Ely, D. H. Reneker, C. A. Tessier and W. J. Youngs, *J. Am. Chem. Soc.*, 2005, **127**, 2285-91

28 S. S. Djokic, *J. Electrochem. Soc.*, 2004, **151,** C359-C364.

29 D. Dellasega, A. Facibeni, F. Di Fonzo, M. Bogana, A. Polissi, C. Conti, C. Ducati, C. S. Casari, A. Li Bassi and C. E. Bottani, *Nanotechnology*, 2008**, 19,** 475602.

30 J. Zhao, W. Zhang and G. Wang, *US Pat. App*, **2007**, 0042052.

31 S. Pal, E. J. Yoon, Y. K. Tak, E. C. Choi and J. M. Song, *J. Am. Chem. Soc.*, 2009, **131**, 16147-16155.

32 Z. A Zatko and J. W. Prather-II, *J Electron SpectroscRelatPhenom*, 1973, **2**, 191-197.

33 D. P. Murtha and R. A. Walton, *Inorg.Chem.*, 1973, **12,** 368-372.

34 S. Pal, Y. K. Tak and J. M. Song. *Appl. Environ. Microbiol.*, 2007, **73**, 1712-1720.

35 S. Pal, E. J. Yoon, S. H. Park, E. C. Choi and J. M. Song, *J. Antimicrob. Chemother.*, 2010, **65,** 2134–2140.

36 J. J. Hostynek, R. S. Hinz and C. Lorence, *Crit. Rev. Toxicol.*, 1993, **23**, 171-235.

37 M. A. Hollinger, *Crit. Rev. Toxicol.*, 1996, **26**, 255-260.

38 J. C. Jiller, C. J. Liao, K. Lewis and A. M. Klibanov, *Proc. Natl. Acad. Sci. U. S. A.*, 2001, **98,** 5981-5985.

39 M. J. Nerurkar, G. M. Zentner and J. H. Rytting, *J. Controlled Release*, 1995, **33**, 357-363.

40 R. H. Skabo and P. W. Smith, *Aust. J. Chem.*, 1969, **22,** 659-661.

41 P. V. Babykutty, C. P. Prabhakaran, R. Anantaraman and C. G. R. Nair, *J. Inorg. Nucl. Chem.*, 1974, **36,** 3685-3688.

42 X. Huang, C. S. Atwood, R. D. Moir, Hartsborn, J. P. Vonsattel, R. E. Tanzi and A. I. Bush, *J. Biol. Chem.*, 1997, **272**, 26464-26470.

43 M. C. Manning and R.W. Woody, *Biopolymers*, 1991, **31**, 569-586.

44 S. Silver, *FEMS Microbiol. Rev.*, 2003, **27**, 341-353.

45 A. Gupta, M. Maynes and S. Silver, *Appl. Environ. Microbiol.*, 1998, **64,** 5042-5045.

46 T. Xu, E. Telser, R. F. Troxler and F. G. Oppenheim, *J. Dent. Res.*, 1990, **69,** 1717–1723.

47 J. Von Haussen, R. Koczulla, R. Shaykhiev, C. Herr, O. Pinkenburg, D. Reimer, R. Wiewrodt, S. Biesterfeld, A. Aigner, F. Czubayko and R. Bals, *Lung Cancer*, 2008, **59,** 12–23.

48 F. Niyonsaba, H. Ushio, N. Nakano, W. Ng, K. Sayama, K. Hashimoto, I. Nagaoka, K. Okumura and H. Ogawa, *J. Invest. Dermatol.*, 2008, **127,** 594–604.

49 G. S. Tjabringa, J. Aarbiou, D. K. Ninaber, J. W. Drijfhout, O. E. Sørensen, N. Borregaard, K. F. Rabe and P. S. Hiemstra, *J. Immunol.*, 2003, **171,** 6690–6696.

50 S. Tokumaru, K. Sayama, Y. Shirakata, H. Komatsuzawa, K. Ouhara, Y. Hanakawa, Y. Yahata, X. Dai, M. Tohyama, H. Nagai, L. Yang, S. Higashiyama, A. Yoshimura, M. Sugai and K. Hashimoto, *J. Immunol.*, 2005, **175,** 4662–4668.

Tables

Table 1. MICs and MBCs (mg/L) of chlorhexidine, silver nitrate, [Ag(I)CHX], [Ag(II)CHX], and silver sulfadiazine by the broth dilution

Strain	Gram Stain	CHX			$AgNO_3$			[Ag(II)CHX]			Hst1 (5 μM) + [Ag(II)CHX]			Silver sulfadiazine
		MIC	MBC	R[a]	MIC	MBC	R[a]	MIC (values in μM)	MBC	R[a]	MIC	MBC	R[a]	MIC
Acinetobacter calcoaceticus (ATCC 23055)	G-	1	1	1	16	16-32	1-2	0.12 (0.18)	0.12	1	1	2	2	4-16
Citrobacter freundii (ATCC 6750)	G-	8	8	1	8	8	1	1-2 (1.5-3)	2	1-2	2	2	1	6.25-50
Enterococcus faecalis (ATCC 29212)	G+	4	4	1	16	16-32	1-2	2 (3)	2	1	2	2	1	50-100
Klebsiella pneumonia (ATCC 10031)	G-	8	8	1	8	8	1	0.5 (0.75)	0.5-1	1-2	0.5	0.5-1	1-2	12.5-100
Propionibacterium acne (ATCC 6919)	G+	2	4	2	8	16	2	0.5 (0.75)	0.5	1	2	2	1	124
Pseudomonas aeruginosa (ATCC 27853)	G-	16	32	2	8	8	1	2 (3)	2	1	2	2-4	1-2	6.25-50
Staphylococcus epidermidis (ATCC 12228)	G+	2	2	1	16	16	1	0.25 (0.38)	0.25	1	1	2	2	6.25-50
Staphylococcus aureus (ATCC 25923)	G+	4	4	1	16	16	1	0.5 (0.75)	0.5	1	1-2	2	1-2	25-100
MRSA(Methicillin-resistant Staphylococcus aureus)	G+	-	-	-	-	-	-	1 (1.5)	1	1	1	1-2	1-2	-
MRCNS(Methicillin-resistant coagulase negative staphylococcus)	G+	-	-	-	-	-	-	0.5-1 (0.75-1.5)	1	1-2	1	1-2	1-2	-

[a] MBC / MIC [b] MIC values obtained using the agar dilution method

Figure Legends:

Figure1. Schematic representation of the synthetic scheme of [Ag(II)CHX] (a) FTIR; (b) and ^{1}H NMR spectra (c) of chlorhexidine (CHX) and [Ag(II)CHX]; (d) X-ray photoelectron spectrum of [Ag(II)CHX] .

Figure 2. Circular dichroism spectra of histatin-1 a function of TFE concentration (a); [Ag(II)CHX] concentration in 20 mM phosphate buffer at pH 7 (b) and in 50% TFE (c); and CD spectra of equimolar (20 μM) conjugate of Hst-1-[Ag (II) CHX] as a function of TFE concentration (d). The experimental conditions are reported under Materials and Methods section.

Figure 3. Representative micrographs (a, b) and graphical representation of results (c, d) of *in vitro* cell-spread assays. Cells were supplemented with different amount of active agents and microscopic images were captured at different time interval. Solid lines in images (a, b) represent cell-free gap boundaries at 0 h. Relative cell-free area (RG_t) (c), and relative spreading (RS_t) (d) at a given time *t* were calculated by quantifying the cell-free area from the micrographs Data represent means ± sd; $n = 10$. $^{*}P<0.01$ *vs*. appropriate control.

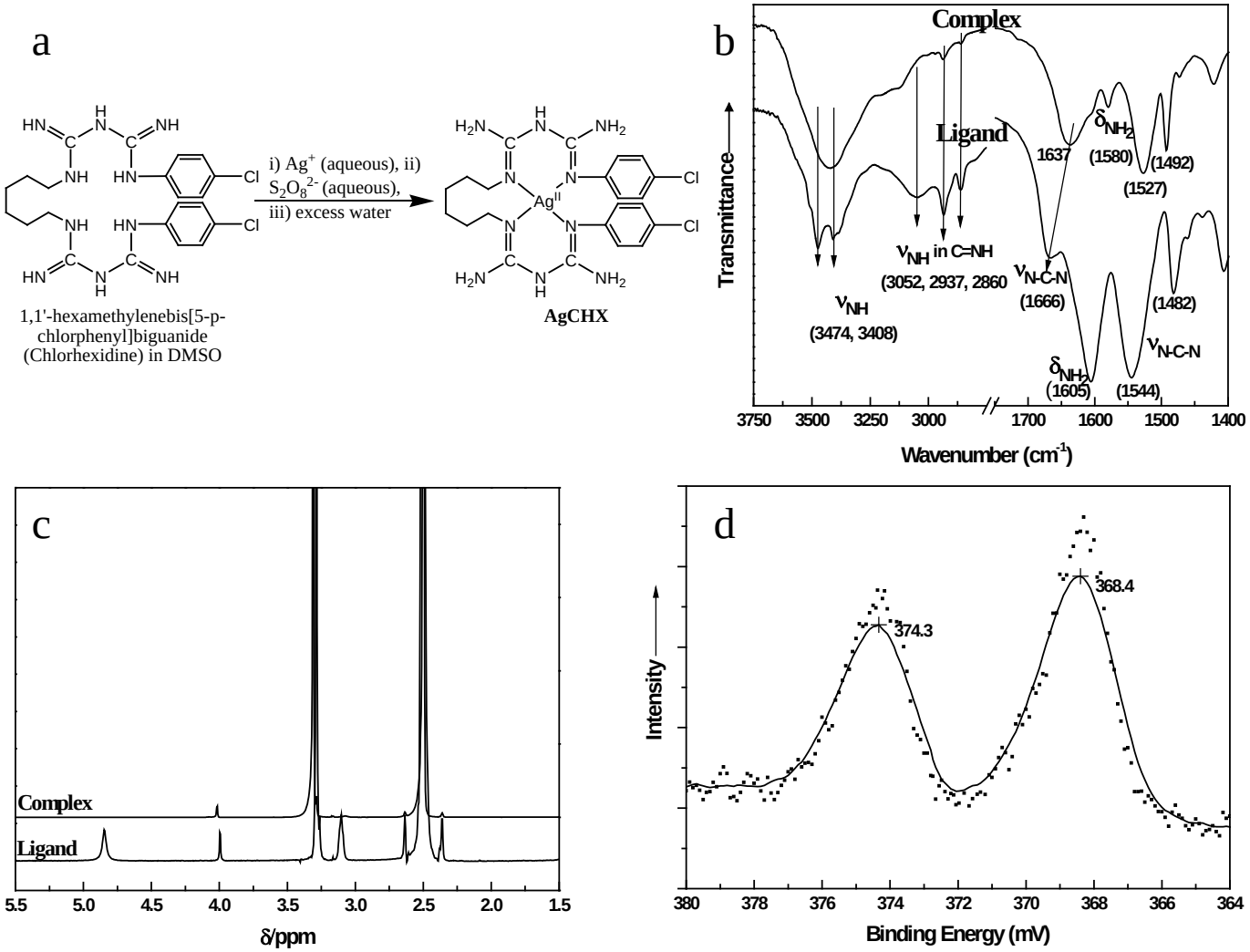

Figure 21

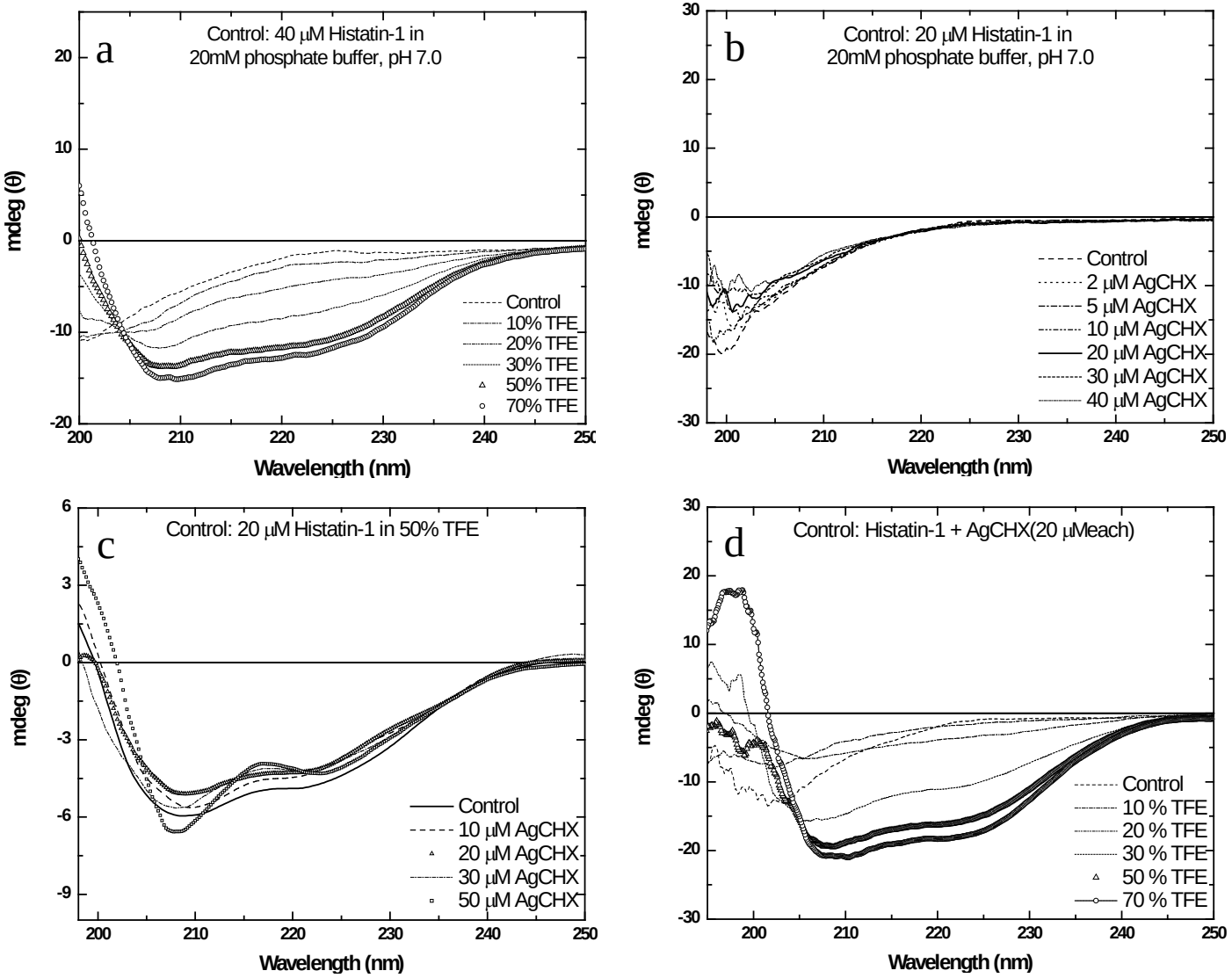

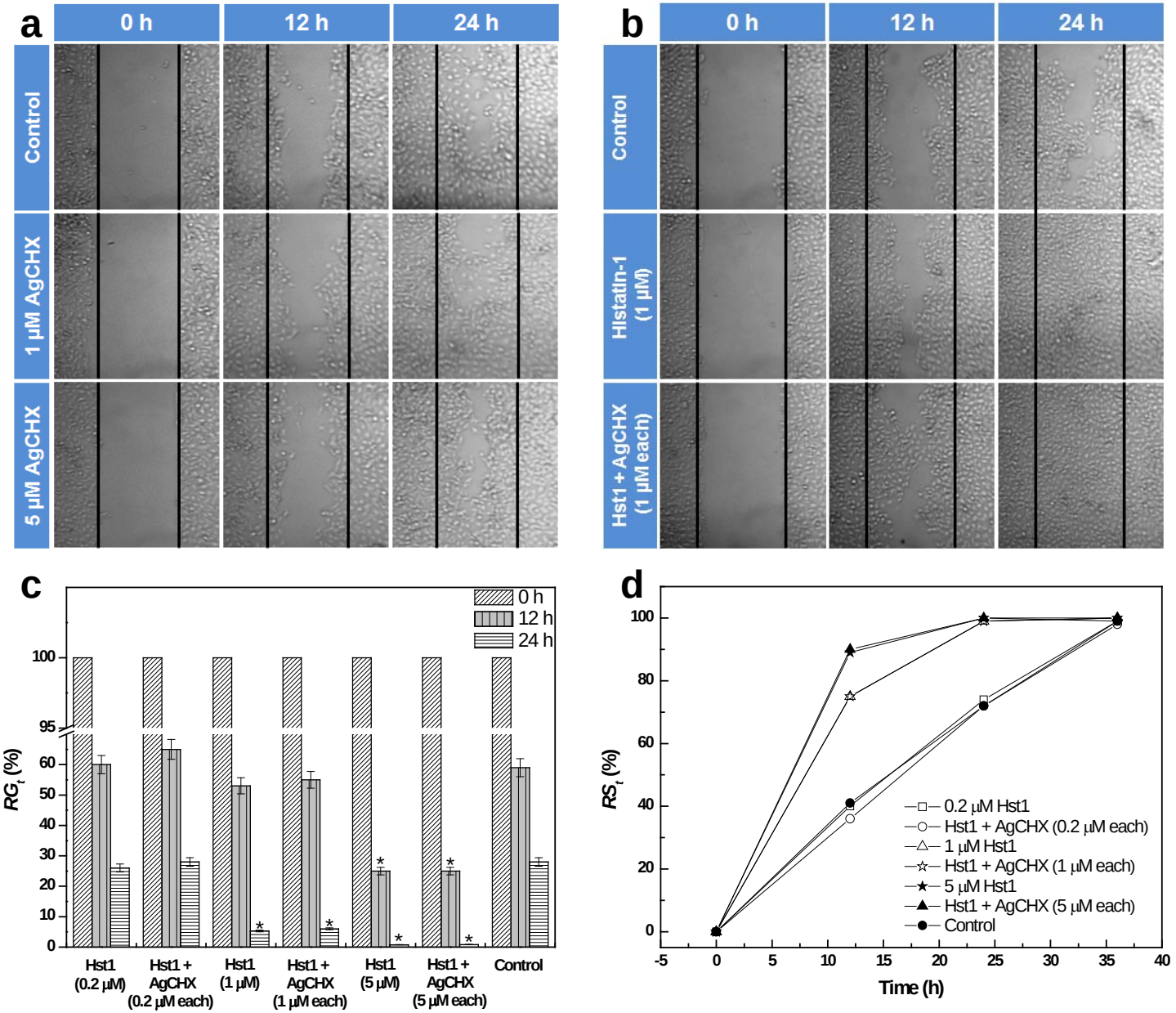

TOC Entry:

Art work:

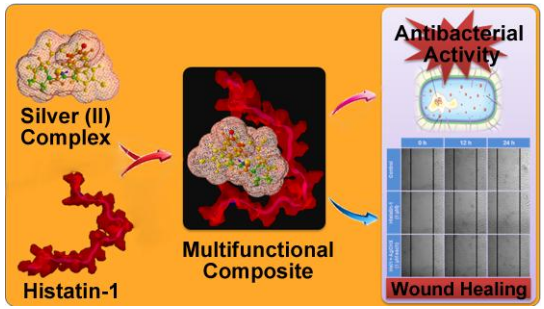

Text: Histatin-1and silver (II) polydiguanide complex composite demonstrated both antibacterial and wound healing promoting activity